

Andreev reflection under high magnetic fields in ferromagnet-superconductor nanocontactsS. Sangiao,^{1,2} J. M. De Teresa,^{1,2,3} M. R. Ibarra,^{1,2} I. Guillamón,⁴ H. Suderow,⁴ S. Vieira,⁴ and L. Morellón^{1,2}¹*Departamento de Física de la Materia Condensada, Universidad de Zaragoza, E-50009 Zaragoza, Spain*²*Laboratorio de Microscopías Avanzadas (LMA), Instituto de Nanociencia de Aragón (INA), Universidad de Zaragoza, E-50018 Zaragoza, Spain*³*Instituto de Ciencia de Materiales de Aragón (ICMA), CSIC-Universidad de Zaragoza, E-50009 Zaragoza, Spain*⁴*Laboratorio de Bajas Temperaturas, Departamento de Física de la Materia Condensada, Instituto de Ciencia de Materiales Nicolás Cabrera, Facultad de Ciencias, Universidad Autónoma de Madrid, E-28049 Madrid, Spain*

(Received 9 November 2011; published 2 December 2011)

We study the magnetic-field dependence of the conductance in planar ferromagnet-superconductor nanocontacts created with focused-electron/ion-beam techniques. From the fits of the differential conductance curves in high magnetic fields, we obtain the magnetic field dependences of the superconducting gap and the broadening parameter. Orbital depairing is found to be linear with magnetic field. We evaluate the magnetic field dependence of the quasiparticle density of states, and we compare it with the value obtained by scanning tunneling spectroscopy experiments.

DOI: [10.1103/PhysRevB.84.233402](https://doi.org/10.1103/PhysRevB.84.233402)

PACS number(s): 74.45.+c, 74.25.F-, 74.78.-w, 81.07.Lk

The study of the differential conductance (that is the first derivative of the I-V characteristic, dI/dV) of point contacts has been demonstrated to be an effective tool to probe the interaction mechanisms in conductive materials: inelastic scattering of electrons by phonons,¹ scattering of electrons by magnons,² etc. If one of the electrodes forming the point contact is superconductor, through the study of the Andreev reflection³ (AR) occurring at the interface it is possible to obtain information on the superconducting gap. In ferromagnet-superconductor point contacts, along with the information on the superconductor gap, the ferromagnet spin polarization can be extracted,^{4,5} making this type of study very appealing.

The superconductor density of states under magnetic field is a relevant parameter in basic studies of superconductivity as well as in applications where the superconductor is under the influence of high magnetic fields. AR measurements in a magnetic field provide further information on the properties of the superconducting⁶ and ferromagnetic electrodes of the contact. So far no systematic investigations of ferromagnet-superconductor nanocontacts under high magnetic fields have been carried out. A comprehensive study of the effect of a magnetic field on the transport properties of ferromagnet-superconductor nanocontacts is due to Pérez-Willard *et al.*,⁷ and the maximum magnetic field applied in this study is 16.5 mT, since the critical field of the Al electrode used as the superconducting electrode is 15 mT. In this Brief Report, we propose a different approach to evaluate the magnetic-field dependence of the quasiparticle density of states of superconductors from the measurement of the conductance in high magnetic fields.

The nanocontacts are created between a superconducting W nanodeposit and a magnetic Co nanodeposit under high vacuum conditions using commercial dual beam equipment that integrates a focused electron column and a focused Ga ion column forming 52 degrees. Focused-electron-beam-induced deposition of magnetic Co (FEBID-Co) and focused-ion-beam-induced deposition of superconducting W (FIBID-W) are made following previous work.^{8–10} Nanocontacts are

obtained by suitably nanoshaping the Co-based magnetic deposit into a sharp tip-like structure, contacting the W-based superconductor. Importantly, the two electrodes forming the contact are grown under high vacuum, minimizing oxidation during contact formation. The *in situ* monitoring of the resistance by means of four electrical microprobes while the nanocontact is being formed allows us to tune very precisely the final room-temperature resistance of the nanocontacts. For *ex situ* transport measurements, four external metallic pads of 5 μm in width are previously micropatterned on the insulating substrate with standard optical lithography techniques. These pads are connected to the nanocontact by four FIBID-Pt nanodeposits of 10 μm in length, connected in such a way that the voltage drop measured is composed of the voltage drop across the nanocontact and the voltage drop across a portion of the superconducting electrode R_{W-e} , as shown in Fig. 1(a). R_{W-e} vanishes below the critical parameters (critical temperature T_C , critical current I_C , and upper critical field B_{C2}) of the W-based superconducting nanodeposit, which is an extreme type-II superconductor following closely simple *s*-wave BCS theory.¹¹ The FIBID-Pt nanodeposits are grown first and the FIBID-W electrode afterwards. The FEBID-Co electrode is grown in the last step and is never irradiated by the Ga ions, which warrants its high-quality magnetic and transport properties. The nanocontacts obtained in this way are stable and reproducible, as reported in a previous publication.¹²

In this Brief Report, we discuss the results obtained in a Co-W nanocontact with a low-temperature resistance of 160 Ω . Figure 1(b) shows the resistance of the nanocontact as a function of perpendicular magnetic field at 2 K for two different currents. Superconducting features disappear in the superconducting W-based nanodeposit around 8.5 T for $I = 50$ nA and around 4.3 T for $I = 10$ μA . Note that, at 50 nA, the voltage drop across the nanocontact is very small, ~ 3.2 μV , much lower than the superconducting gap (0.7 meV) and thus, the electrons that meet the interface between the ferromagnet and the superconductor can be Andreev reflected. This results in an increase of the resistance at low fields, because the spin imbalance in the ferromagnet

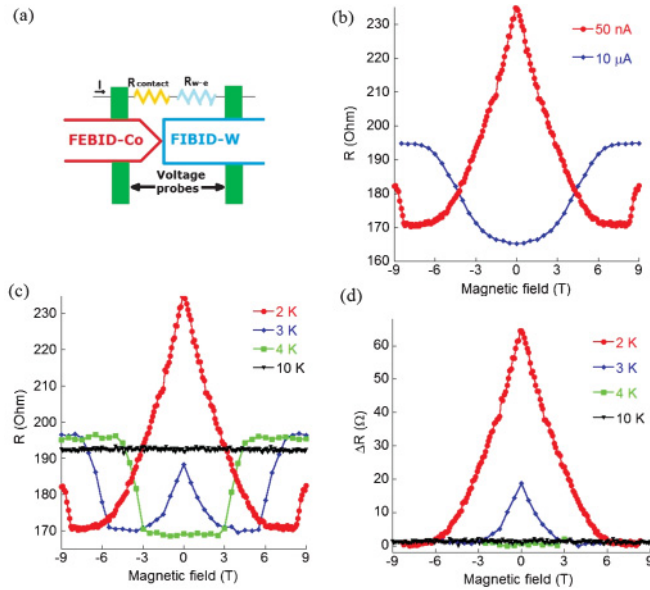


FIG. 1. (Color online) (a) Sketch of the voltage drop measured in the nanocontacts. It is composed of the voltage drop across the nanocontact and the voltage drop across a portion of the superconducting electrode R_{W-e} . (b) Resistance of the nanocontact as a function of perpendicular magnetic field at 2.0 K for two different currents. (c) Resistance of the nanocontact as a function of perpendicular magnetic field at different temperatures for an applied current of 50 nA. (d) Change in resistance (relative to the value just below the resistive transition) with the applied perpendicular magnetic field at different temperatures for an applied current of 50 nA.

at the Fermi level limits the Andreev transport across the nanocontact. The resistance decreases as the magnetic field is increased due to the change in the density of states of the superconductor induced by the application of a high magnetic field. Interestingly, the polarization of the ferromagnetic electrode remains unchanged.

As the W-based electrode is a type-II superconductor, when applying 10 μ A, we observe the flow of vortices in the superconducting nanodeposit and a rounded increase in the resistance, in the presence of an external magnetic field applied perpendicular to the superconducting film surface. The Lorentz force tends to move the vortices perpendicular to the current, giving rise to a dissipation.¹³ Thus, the application of increasingly high magnetic field results in a monotonous enhancement of the resistance before reaching the normal state.

We have investigated the evolution of the magnetoresistance with temperature. Figures 1(c) and 1(d) show the magnetic-field dependence of the resistance with a current of 50 nA at different temperatures below and above the critical temperature of the superconducting electrode (5.1 K for an applied current of 50 nA). The high magnetoresistance ratio, defined as $MR(B) = 100 \times [R(B) - R(0)]/R(0)$, observed at high fields at 2 K ($MR \approx -27\%$ at 6 T) decreases rapidly at higher temperatures. The reason for this decrease in the MR ratio is that the number of states available in the superconductor is enhanced with the increase of temperature, and the enhancement of the number of states available results

in a decrease of the resistance. At temperatures above 4 K, the resistance remains constant until it increases sharply at the upper critical field. As the current is smaller, no effects due to vortex motion are observed, and leads to a sharp resistive transition. Vortex flow does not play any role either in the differential conductance, because in the nanocontacts studied the contact area has a diameter of few nanometers. We expect the contact region to be vortex free, simply because the contact area is too small to hold a flux quantum at the fields of the measurements shown here. Regarding this matter, the nanocontacts studied here are very different from the point contacts studied by Miyoshi *et al.*¹⁴ The latter ones have a contact area of 10 μ m in diameter and, as a result, the effect of normal vortex cores in the superconductor on the transport across the interface is very pronounced.

To extract the differential conductance as a function of the bias voltage, the current versus voltage characteristics of the nanocontact have been measured at different temperatures and magnetic fields applied perpendicular to the plane of the nanocontact. The temperature dependence of these conductance curves at zero magnetic field has been previously investigated¹² and analyzed using the model proposed by Blonder, Tinkham, and Klapwijk (BTK)^{15,16} for a contact between a normal metal and a superconductor, extended to include the spin polarization of the ferromagnetic metal. From the analysis of the conductance curves, we obtained information on the superconducting gap Δ , the ferromagnet spin polarization P , and the dimensionless parameter Z that results from representing the interface scattering by a repulsive δ -function potential of strength Z . In this Brief Report, we focus on the magnetic-field dependence of the conductance curves and analyze them to obtain quantitative information on the magnetic-field dependence of the relevant properties of the superconducting electrode.

The application of a magnetic field breaks the time-reversal symmetry of the Cooper-pair condensate, which gives rise to the pair-breaking effect. It has been shown¹⁷ that the orbital depairing produced by the magnetic field can be considered by including in the extended BTK theory a single broadening parameter Γ in the form of an imaginary part of the energy, i.e., $E \rightarrow E + i\Gamma$. Introducing Γ in the BCS quasiparticle density of states leads to the modified expression¹⁸

$$N_S(E, \Gamma) = \text{Re} \left[\frac{(E - E_F) + i\Gamma}{\sqrt{[(E - E_F) + i\Gamma]^2 - \Delta^2}} \right], \quad (1)$$

where N_S is normalized at the value in the normal state. Γ enters the BTK model through the BCS quasiparticle and pair densities of states and modifies the resulting BTK conductance so that its amplitude is lowered and its energy is broadened. Γ adds small lifetime corrections to the BCS value of the superconductor density of states.¹⁹

In Fig. 2, the differential conductance obtained for the nanocontact at 2 K and applying different magnetic fields perpendicular to the plane of the nanocontact is shown. The conductance values have been normalized to the value of the conductance in the normal state subtracting the voltage drop across R_{W-e} . The solid lines displayed in Fig. 2 are the best fits obtained to the extended BTK model, including the single broadening parameter Γ through the BCS quasiparticle

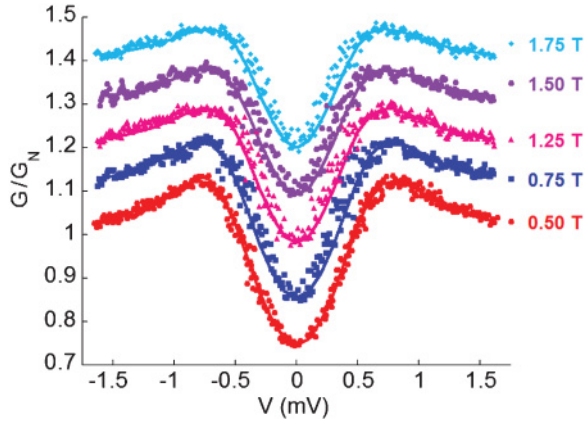


FIG. 2. (Color online) Bias-voltage dependence of the normalized differential conductance at 2 K and applying different magnetic fields perpendicular to the plane of the nanocontact. For clarity, each curve has been shifted upward by 0.1 with respect to that immediately below. The solid lines are the conductance curves obtained from fits to the extended BTK model including the single broadening parameter Γ .

[Eq. (1)] and pair density of states. In these fits, the spin polarization of the ferromagnet P and the barrier strength Z have been treated as fully free parameters but found to have the same values as those previously obtained in the fits of the conductance curves measured at the same temperature at zero magnetic field [for this nanocontact, $P = 0.356(6)$ and $Z = 0.07(1)$, both parameters are also independent of temperature], thus, the only two adjustable parameters in the fitting process are the superconducting gap Δ and the single broadening parameter Γ .

Figure 3 shows the values of Δ and Γ obtained from fits of the differential conductance to the extended BTK model that includes the pair-breaking effect of the magnetic field through Γ . Both parameters exhibit a linear dependence with the magnetic field, Δ decreases linearly as the magnetic field is increased in the magnetic field range up to 2 T in which we have fitted the experimental conductance curves and Γ increases linearly. Γ at all magnetic field values verifies $\Gamma \ll \Delta$ and at the lowest fields measured is nearly zero, indicating that the intrinsic (field-independent) broadening parameter is negligible, so it can be concluded that the inelastic scattering is not playing any role in the transport across the interface. The negligible values obtained for Γ at low fields also indicate that spin-orbit scattering, and thus the lifetime for spin mixing arising from spin-orbit scattering, is not contributing significantly to Γ . The orbital depairing parameter ζ can be consequently calculated from Δ and Γ as $\zeta = \Gamma/\Delta$. As shown in the inset of Fig. 3, ζ increases linearly as a function of the magnetic field, as expected for a type-II superconductor if only orbital depairing is contributing to Γ .²⁰

We have obtained the magnetic-field dependence of the quasiparticle density of states by introducing the dependences of the superconducting gap and the broadening parameter on the applied magnetic field, obtained from the fits of the conductance curves at different magnetic fields, in Eq. (1). We have compared the results obtained in our fabricated nanojunctions with scanning tunneling spectroscopy. These

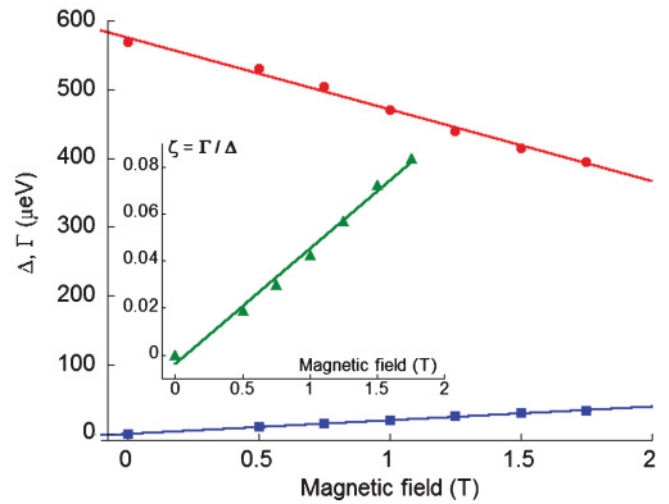


FIG. 3. (Color online) Superconducting gap (dots) and broadening parameter (squares) values obtained from fits of the differential conductance to the extended BTK model. The solid lines are fits to a linear dependence. The inset shows the magnetic-field dependence of the orbital depairing parameter $\zeta = \Gamma/\Delta$ and its fit to a linear dependence.

measurements, shown in the inset of Fig. 4, were performed on a 200-nm-thick FIBID-W nanodeposit grown at the center of a conducting Au layer previously deposited on a Si substrate, and the magnetic field was applied perpendicular to the sample surface, that is the same direction in which the magnetic field was applied in the AR measurements. The sample was mounted in a low-temperature scanning tunneling microscope (STM) thermally anchored to the mixing chamber of a dilution refrigerator (for a more detailed description of the experimental setup, see Ref. 21). As can be seen in

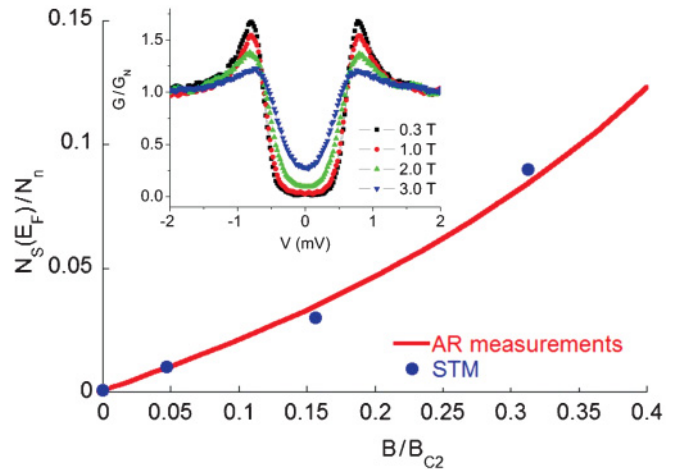


FIG. 4. (Color online) Magnetic-field dependence of the quasi-particle density of states. The dots correspond to the density of states measured by STM, and the line corresponds to the dependence obtained by introducing the magnetic-field dependences of the superconducting gap and the broadening parameter in Eq. (1) to evaluate the density of states. Inset: Normalized differential tunneling conductance as a function of the bias voltage measured by STM for different magnetic fields perpendicular to the superconducting W-FIBID nanodeposit.

Fig. 4, the values of the density of states obtained through AR measurements and its magnetic-field dependence are in good agreement with the ones measured by scanning tunneling spectroscopy. We observe a smooth variation of the density of states with the magnetic field with a slope lower than one. A higher value of this slope is expected at magnetic fields close to the upper critical field. It is also remarkable that an orbital depairing parameter linear in the magnetic field gives a density of states at the Fermi level that is nonlinear in the magnetic field.

In conclusion, we have developed a specific approach for determining the density of states of superconductors in high magnetic fields through the study of the magnetic-field dependence of the conductance. We have validated the results obtained using this approach by comparing these results to the direct measurement of the density of states as a function of the magnetic field by scanning tunneling spectroscopy, obtaining strong experimental evidence for the reliability of

our approach. This study of the conductance in ferromagnet-superconductor nanocontacts up to high magnetic fields has been possible due to the large upper critical field of the superconducting FIBID-W nanodeposit, making it suitable and very promising for a wide range of applications in nanoscale superconductivity. It is worth noting that this study is also feasible in any other superconducting and/or ferromagnetic material by implementing a previous lithographic step.

This work was supported by the Spanish Ministry of Science (through projects MAT2008-06567-C02, including FEDER funding) and the Aragón Regional Government (project E26). S. Sangiao acknowledges financial support from Spanish MEC. We acknowledge Rosa Córdoba for the growth of the sample used for the scanning tunnelling spectroscopy measurements and Javier Sesé for discussions on superconducting W nanodeposits.

-
- ¹I. K. Yanson, Zh. Eksp. Teor. Fiz. **66**, 1035 (1974) [Sov. Phys. JETP **39**, 506 (1974)].
- ²A. M. Duif, A. G. M. Jansen, and P. Wyder, *J. Phys. Condens. Matter* **1**, 3157 (1989).
- ³A. F. Andreev, Zh. Eksp. Teor. Fiz. **46**, 1823 (1964) [Sov. Phys. JETP **19**, 1228 (1964)].
- ⁴R. J. Soulen, J. M. Byers, M. S. Osofsky, B. Nadgorny, T. Ambrose, S. F. Cheng, P. R. Broussard, C. T. Tanaka, K. Nowak, J. S. Moodera, A. Barry, and J. M. D. Coey, *Science* **282**, 85 (1998).
- ⁵S. K. Upadhyay, A. Palanisami, R. N. Louie, and R. A. Buhrman, *Phys. Rev. Lett.* **81**, 3247 (1998).
- ⁶P. Szabó, P. Samuely, J. Kacmarcik, T. Klein, J. Marcus, D. Fruchart, S. Miraglia, C. Marcenat, and A. G. M. Jansen, *Phys. Rev. Lett.* **87**, 137005 (2001).
- ⁷F. Pérez-Willard, J. C. Cuevas, C. Sürgers, P. Pfundstein, J. Kopu, M. Eschrig, and H. v. Löhneysen, *Phys. Rev. B* **69**, 140502(R) (2004).
- ⁸A. Fernández-Pacheco, J. M. De Teresa, R. Córdoba, and M. R. Ibarra, *J. Phys. D: Appl. Phys.* **42**, 055005 (2009).
- ⁹L. Bernau, M. Gabureac, and I. Utke, *Angewandte Chemie International Edition* **49**, 8880 (2010).
- ¹⁰J. M. De Teresa, A. Fernández-Pacheco, R. Córdoba, J. Sesé, M. R. Ibarra, I. Guillamón, H. Suderow, and S. Vieira, *Mater. Res. Soc. Symp. Proc.* **1180**, CC04-09 (2009).
- ¹¹I. Guillamón, H. Suderow, S. Vieira, A. Fernández-Pacheco, J. Sesé, R. Córdoba, J. M. De Teresa, and M. R. Ibarra, *New J. Phys.* **10**, 093005 (2008).
- ¹²S. Sangiao, L. Morellón, M. R. Ibarra, and J. M. De Teresa, *Solid State Commun.* **151**, 37 (2011).
- ¹³Y. B. Kim, C. F. Hempstead, and A. R. Strnad, *Phys. Rev. A* **139**, 1163 (1965).
- ¹⁴Y. Miyoshi, Y. Bugoslavsky, and L. F. Cohen, *Phys. Rev. B* **72**, 012502 (2005).
- ¹⁵G. E. Blonder, M. Tinkham, and T. M. Klapwijk, *Phys. Rev. B* **25**, 4515 (1982).
- ¹⁶G. E. Blonder and M. Tinkham, *Phys. Rev. B* **27**, 112 (1983).
- ¹⁷Yu. G. Naidyuk, R. Häussler, and H. v. Löhneysen, *Physica B* **218**, 122 (1996).
- ¹⁸R. C. Dynes, V. Narayanamurti, and J. P. Garno, *Phys. Rev. Lett.* **41**, 1509 (1978).
- ¹⁹D. C. Worledge and T. H. Geballe, *Phys. Rev. B* **62**, 447 (2000).
- ²⁰K. Maki, in *Superconductivity*, edited by R. D. Parks (M. Dekker, New York, 1969), Vol. 2, p. 1035.
- ²¹H. Suderow, I. Guillamón, and S. Vieira, *Rev. Sci. Instrum.* **82**, 033711 (2011).